Reactive Polymer Coatings: A Platform for Patterning Proteins and Mammalian Cells onto a Broad Range of Materials

Jörg Lahann,[†] Mercedes Balcells,[†] Teresa Rodon,[†] Jinwook Lee,[†] Insung S. Choi,[‡] Klavs F. Jensen,[†] and Robert Langer*,[†]

Department of Chemical Engineering, Massachusetts Institute of Technology, Cambridge, Massachusetts 02139, and Department of Chemistry, School of Molecular Science—BK21 and Center for Molecular Design and Synthesis, Korea Advanced Institute of Science and Technology, Daejeon 305-701, Korea

Received September 21, 2001. In Final Form: January 14, 2002

We report a procedure for surface modification based on chemical vapor deposition polymerization of functionalized [2.2]paracyclophanes that is essentially substrate-independent. Poly(*p*-xylylene-2,3-dicarboxylic anhydride) and poly[*p*-xylylene carboxylic acid pentafluorophenolester-*co*-*p*-xylylene] are examined as templates for cell patterning. Both reactive coatings are deposited on poly(tetrafluoroethylene), polyethylene, silicon, gold, stainless steel, and glass and show excellent adhesion when deposited in thin films (ca. 100 nm) under optimized polymerization conditions. X-ray photoelectron spectroscopy and grazing angle infrared spectroscopy have been used to confirm chemical homogeneity in both cases. Reactive coatings are subsequently patterned by microcontact printing of an amino-terminated biotin ligand and serve as templates for layer-by-layer self-assembly. Streptavidin selectively binds to the biotin-exposing surface regions and allows surface confinement of a biotin-tethered antibody against α_5-integrin. The specific interaction of this antibody with endothelial cells results in spatially directed deposition of mammalian cells. Fluorescence microscopy is used to verify accurate self-assembly at each step. Although both reactive coatings differ in how they chemically bind biomolecules, their ability to support formation of pattern by microcontact printing is similar.

1. Introduction

Patterned polymer films are used as scaffolds for tissue engineering,[1] components in molecular electronic[2] and optical devices,[3] and as etch resists.[4,5] In addition, surfaces with patterns of conjugates for bioactive molecules, proteins, or cells are important for several technologies such as the development of certain biosensors[6,7] and fundamental studies of cell biology.[8−10]

Patterns of proteins or cells have been generated by means of photolithographic techniques. Examples include the spatially controlled photoablation of previously adsorbed proteins[11] and the linkage of proteins via photosensitive groups.[12] Photolithography however tends to be laborious and expensive.[13,14] Soft lithographic methods[15] were shown to be a versatile technique for generating patterns of proteins[13,16] or various mammalian cells.[13−14] Most of these techniques are restricted to substrates such as gold, silver, or silicon,[17] whereas for many applications, other substrates such as polymers are more desirable. In another approach, polymers were surface-modified via multistep synthesis to generate substrates for microcontact printing (μCP).[18−22] In principle, polymers may be deposited as thin films by spin-coating to provide interfaces for further surface modification.[23]

Alternatively, we prepared polymer films deposited by chemical vapor deposition (CVD) polymerization that can provide an essentially substrate-independent platform for surface modification.[24,25] Its simplicity in providing a wide

* To whom correspondence should be addressed: E-mail: rlanger@mit.edu. Fax: 617-258-8827.

[†] Massachusetts Institute of Technology.

[‡] Korea Advanced Institute of Science and Technology.

(1) Gosh, P.; Amirpour, M. L.; Lackowski, W. M.; Pishko, M. V.; Crooks, R. M. *Angew. Chem., Int. Ed.* **1999**, *38*, 1592.
(2) MacDonald, S. A.; Willson, C. G.; Frechet, J. M. J. *Acc. Chem. Res.* **1994**, *27*, 151.
(3) Healy, B. G.; Foran, S. E.; Walt, D. R. *Sience* **1995**, *269*, 1078.
(4) Zamborini, F. P.; Crooks, R. M. *Langmuir* **1997**, *13*, 122.
(5) Jeon, N. L.; Choi, I. S.; Whitesides, G. M.; Kim, N. Y.; Laibinis, P. E.; Harada, Y.; Finnie, K. R.; Girolami, G. S.; Nuzzo, R. G. *Appl. Phys. Lett.* **1999**, *75*, 4201.
(6) Crooks, R. M.; Ricco, A. J. *Acc. Chem. Res.* **1998**, *31*, 219.
(7) Mrksich, M.; Whitesides, G. M. *Trends Biotechnol.* **1995**, *12*, 228.
(8) Jung, D. R.; Cuttino, S.; Pancrazio, J. J.; Manos, P.; Cluster, T.; Sathanoori, R. S.; Aloi, L. E.; Coulombe, M. G.; Czarnaski, M. A.; Borkholder, D. A.; Kovacs, G. T. A. Bey, P.; Stenger, D. A.; Hickman, J. J. *J. Vac. Sci. Technol.* **1998**, *16*, 1183.
(9) Singhvi, R.; Kumar, A.; Lopez, G. P.; Stephanopoulos, G. N.; Wang, D. I. C.; Whitesides, G. M.; Ingber, D. E. *Science* **1994**, *264*, 696.
(10) Chen, C. S.; Mrksich, M.; Huang, S.; Whitesides, G. M.; Ingber, D. E. *Biotechnol. Prog.* **1998**, *14*, 356.
(11) Hammarback, J. A.; Palm, S. L.; Furch, L. T.; Letourneau, P. C. *J. Neurosci. Res.* **1985**, *13*, 213.
(12) Blawas, A. S.; Oliver, T. F.; Pirrung, M. C.; Reichert, W. M. *Langmuir* **1998**, *14*, 4243.
(13) Kane, R. S.; Takayama, S.; Ostuni, E.; Ingber, D. E., Whitesides, G. M. *Biomaterials* **1999**, *20*, 2363.
(14) Mrksich, M.; Dike, L. E.; Tien, J.; Ingber, D. E.; Whitesides, G. M. *Exp. Cell Res.* **1997**, *235*, 305.
(15) Xia, Y.; Whitesides, G. M. *Angew. Chem., Int. Ed.* **1998**, *37*, 550.
(16) Bernard, A.; Renault, J. P.; Michel, B.; Bosshard, H. R.; Delamarche, E. *Adv. Mater.* **2000**, *12*, 1067−1070.
(17) Ulman, A. *Chem. Rev.* **1996**, *96*, 1533.
(18) Patel, N.; Bhandari, R.; Shakesheff, K. M.; Cannizzaro, S. M.; Davies, M. C.; Langer, R.; Roberts, C. J.; Tendler, S. J. B.; Williams, P. M. *J. Biomater. Sci., Polym. Ed.* **2000**, *11*, 319.
(19) Black, F. E.; Hartshorne, M.; Davies, M. C.; Roberts, C. J.; Tendler, S. J. B.; Williams, P. M.; Shakesheff, K. M.; Cannizzaro, S. C.; Kim, I.; Langer, R. *Langmuir* **1999**, *15*, 3157.
(20) Yang, Z.; Chilikoti, A. *Adv. Mater.* **2000**, *12*, 413.
(21) Hyun, J.; Zhu, Y.; Liebmann-Vinson, A.; Beebe, T. P.; Chilkoti, A. *Langmuir* **2001**, *17*, 6358.
(22) Yang, Z.; Belu, A. M.; Liebmann-Vinson, A.; Sugg, H.; Chilkoti, A. *Langmuir* **2000**, *16*, 7482.
(23) Kim, H.; Urban, M. W. *Langmuir* **1998**, *14*, 7235.
(24) Lahann, J.; Klee, D.; Höcker, H. *Macromol. Rapid Commun.* **1998**, *19*, 441.

10.1021/la011464t CCC: $22.00
Published on Web 04/04/2002

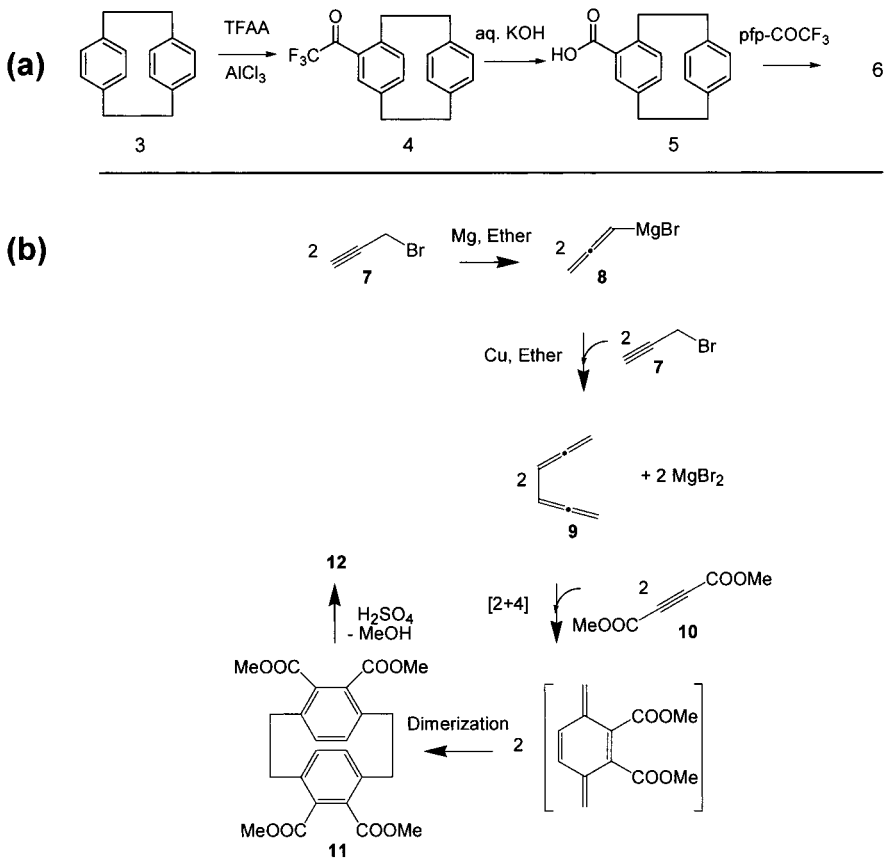

Figure 1. Chemical synthesis of (a) [2.2]paracyclophane pentafluorophenol ester (**6**) and (b) [2.2]paracyclophane 4,5,12,13-tetracarboxylic dianhydride (**12**).

range of functional groups,[24,26] the excellent adhesion to various substrates,[27] and its applicability to devices with three-dimensional geometries[27] appear to be advantageous when compared to polymers deposited by solvent-based methods. In addition, a one-step coating procedure that provides linkable reactive groups without requiring chemical modification of the deposited films is highly desirable. In a previous study, we used CVD polymerization to prepare poly[*p*-xylylene carboxylic acid pentafluorophenol ester-*co*-*p*-xylylene] (**1**), a reactive coating with active ester groups incorporated in the polymer structure, and demonstrated in a basic study its ability to support patterning of small biomolecules by means of μCP.[26] The potential impact of this technology in surface engineering may depend on how variable reactive coatings with different functional groups can be prepared enabling different binding modes for biomolecules. In addition, it might be desirable for certain applications to avoid potentially harmful leaving groups such as pentafluorophenol.[22]

The main motivation of this work is (a) to broaden the platform of reactive coatings by preparing poly(*p*-xylylene-2,3-dicarboxylic anhydride) (**2**), a polymer with functional groups that does not release toxic side-products when reacting with biological target molecules, and (b) to compare this reactive coating with polymer **1** in how accurate biomolecule patterns can be prepared. As a further objective, we studied the interaction of biotin-patterned surfaces with proteins and cells and developed a strategy for spatially directed surface modification based on layer-by-layer self-assembly.

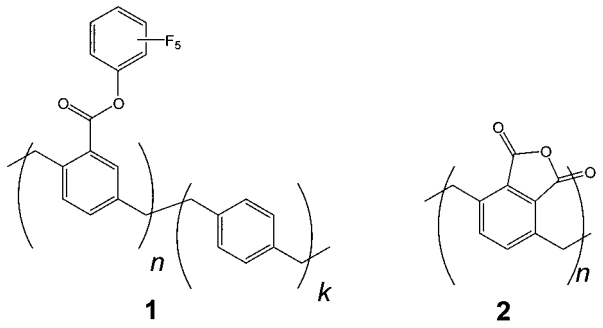

2. Materials and Methods

2.1. Materials. If not indicated differently, chemicals were purchased from Aldrich, Milwaukee, WI, and were used without further purification. PDMS oligomer Sylgard 184 was purchased from Dow Corning. Poly(tetrafluoroethylene) (PTFE), polyethylene (PE), and stainless steel were purchased from Goodfellow (U.K.). (+)-Biotinyl-3,6,9-trioxaundecanediamine, streptavidin, and fluorescein-conjugated streptavidin were purchased from Pierce, USA, and fluorescein-conjugated secondary antibody was purchased from Sigma, USA. Biotin-conjugated human anti-α_5-integrin was purchased from Pharmingen, USA, and bis-benzimide was purchased from Hoechst, Germany. Silicon wafers (Silicon Quest Int., Santa Clara, CA) were either used as purchased or after deposition of a sequence of silicon nitride (200 nm), titanium (10 nm), and gold (100 nm).

2.2. Precursor Synthesis. *[2.2]Paracyclophane Pentafluorophenol Ester (**6**).* Compound **6** was synthesized via a three-step synthesis as described in detail elsewhere.[26] All products were characterized by infrared, nuclear magnetic resonance spec-

(25) Lahann, J.; Höcker, H.; Langer, R. *Angew. Chem., Int. Ed.* **2001**, *40*, 726.
(26) Lahann, J.; Choi, I. S.; Lee, J.; Jensen, K. F.; Langer, R. *Angew. Chem., Int. Ed.* **2001**, *40*, 3166.
(27) Lahann, J.; Plüster, W.; Klee, D.; Höcker, H. *Biomaterials* **2001**, *22*, 817.

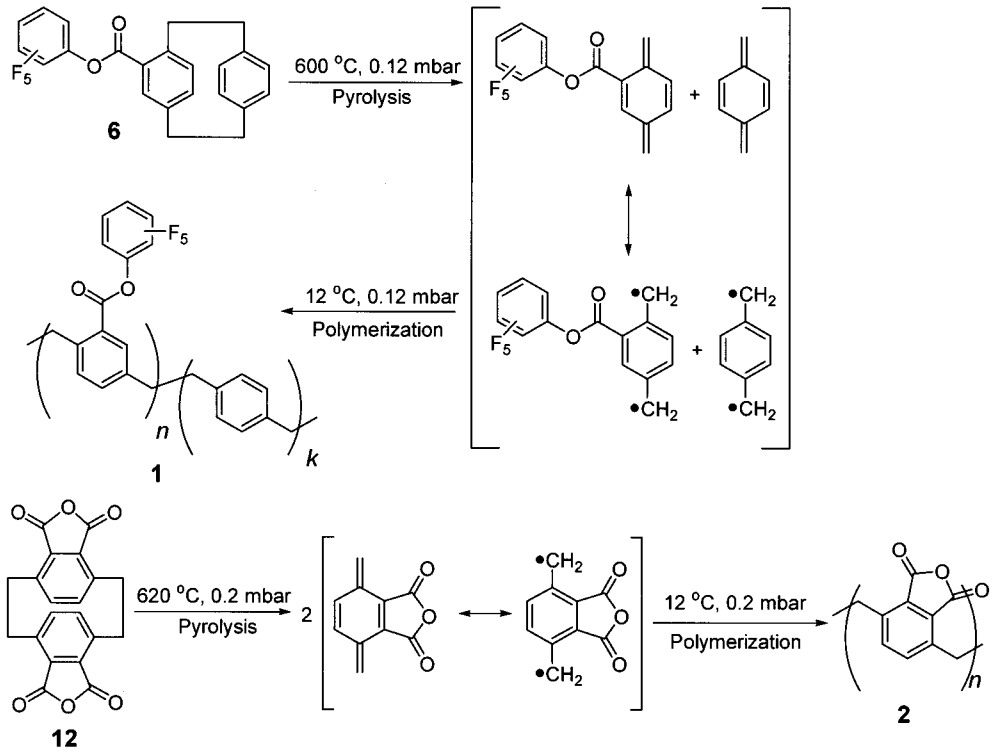

Figure 2. Chemical vapor deposition polymerization to yield polymers **1** and **2**.

Table 1. CVD-Polymerization Parameters Used for Deposition of Reactive Coatings

polymer	sublimation temp (°C)	pyrolysis temp (°C)	precursor (mg)	substrate temp (°C)	system pressure (mbar)	argon mass flow (sccm)[a]	film thickness (nm)
1	230	600	50	12	0.12	2.0	131
2	310	620	36	12	0.2	4.5	90

[a] sccm, standard cubic centimeter.

troscopy (^{1}H and ^{13}C), and mass spectrometry. The spectroscopic data were found to be in accordance with literature data.[26] The purity of **6** was 98.5% as determined by gas chromatography.

*4,5,12,13-Tetrakis(methyloxy carbonyl) [2.2]Paracyclophane (**11**).* Mercury(II) chloride (125 mg, 0.50 mmol) and magnesium (7.3 g, 300 mmol) were heated under an argon atmosphere. Then propargylic bromide (**7**, 1.25 mL, 16 mmol) dissolved in 40 mL of carefully dried diethyl ether was added at room temperature. When the diethyl ether started refluxing, the solution was cooled to 5 °C and compound **7** (22.3 mL, 283 mmol) in 145 mL diethyl ether was added slowly (**Caution**: *Grignard reaction may cause strong heat development!*). Subsequently, the solution was stirred for another 45 min at room temperature and copper(I) chloride (500 mg, 5 mmol) was added. After being stirred for 25 min at room temperature, the solution was cooled to 0 °C and compound **7** (21.3 mL, 270 mmol) dissolved in 25 mL of diethyl ether was added while the solution was kept well below 15 °C. After being stirred for 15 min, the solution was cooled to 0 °C and it was quenched by adding cooled and degassed aqueous HCl (1 N, 50 mL). The organic phase was separated, hydroquinone (80 mg) was added, and the solution was dried for 45 min over potassium carbonate. Distillation at 45 °C using a 30 cm Vigreux column delivered 1,2,4,5-heaxatetraene (**9**). A solution of **7** in diethyl ether was added to a mixture of 15 mL of acetylenedicarboxylic acid dimethyl ester (**10**, 123 mmol) and 55 mL of benzene. The reaction mixture was the stirred for 4 h at 45 °C and for 16 h at 75 °C. White crystals of **11** precipitated and were purified by recrystallization in toluene. ^{1}H NMR ($CDCl_3$/TMS, 300 MHz, ppm): δ = 3.21 (8H, CH_2), 3.86 (s, 12H, CH_3), 6.86 (s, 4H, C*H*). ^{13}C NMR ($CDCl_3$/TMS, 75 MHz, ppm): δ = 33.3 (CH_2), 52.3 (OCH_3), 131.6 (*C*−COO), 135.1 (*C*H), 139.7 (*C*−CH_2), 168.4 (*C*=O). IR (KBr, cm^{-1}): ν = 2952 (m,), 1725 (s), 1544 (m), 1437 (m), 1268 (s), 1197 (m), 1112 (m), 972 (w). MS (70 eV, direct injection), m/z = 440 (M^+), 220 (1/2M^+), 217, 205, 199, 185, 159, 127, 115, 107, 105, 99, 91, 85, 79, 77, 71, 59, 57, 55. Elemental analysis, $C_{24}H_{24}O_8$: C, 65.29% (calcd 65.45%); H, 5.47% (calcd 5.49%); O, 29.10% (calcd 29.06%).

*[2.2]Paracyclophane 4,5,12,13-Tetracarboxylic Dianhydride (**12**).* Compound **12** was synthesized from **11** by reaction with concentrated sulfuric acid for 30 min at 0 °C in yields higher than 92% based on the recovered starting material. IR (KBr, cm^{-1}): 865 (m), 1179 (w), 1757 (s), 1838 (m), 2947 (w), 3059 (w). MS (70 eV, direct injection), m/z = 348 (M^+), 330 ($M^+ - H_2O$), 302 (330 − CO), 274 (302 − CO), 202, 189, 174 ($^1/_2M^+$), 146 (174 − CO), 117, 102 ($C_8H_6^+$), 89 ($C_7H_5^+$), 76 ($C_6H_5^+$), 63. Elemental analysis, $C_{20}H_{12}O_6$: C, 65.97% (calcd 68.97%); H, 3.43% (calcd 3.47%); O, 27.2% (calcd 27.56%).

2.3. CVD Polymerization. Polymers **1** and **2** were obtained from the corresponding [2.2]paracyclophanes **6** and **12** by CVD polymerization using an installation consisting of a sublimation zone, a pyrolysis zone, and a deposition chamber.[26] Polymerization parameters are summarized in Table 1. The pyrolysis of the [2.2]-paracyclophanes was carried out in a furnace with three independently regulated heating zones to ensure a constant temperature profile. The polymerization chamber is equipped with a rotating, cooled sample holder, an on-line thickness monitor (Sycon Instruments, New York), and temperature and vacuum gauges. For polymerization, a defined amount of starting material was placed in the sublimation zone and a substrate was fixed on the sample holder at a particular temperature. A defined argon flow was used as carrier gas, the pressure was adjusted, and the pyrolysis zone was heated. Subsequently, starting material was slowly sublimed by increasing the temperature of the sublimation zone. Polymerization resulted in transparent polymer films on the substrate.

2.4. Surface Characterization. X-ray photoelectron spectroscopy (XPS) data were recorded on an Axis Ultra X-ray photoelectron spectrometer (Kratos Analyticals, USA) equipped

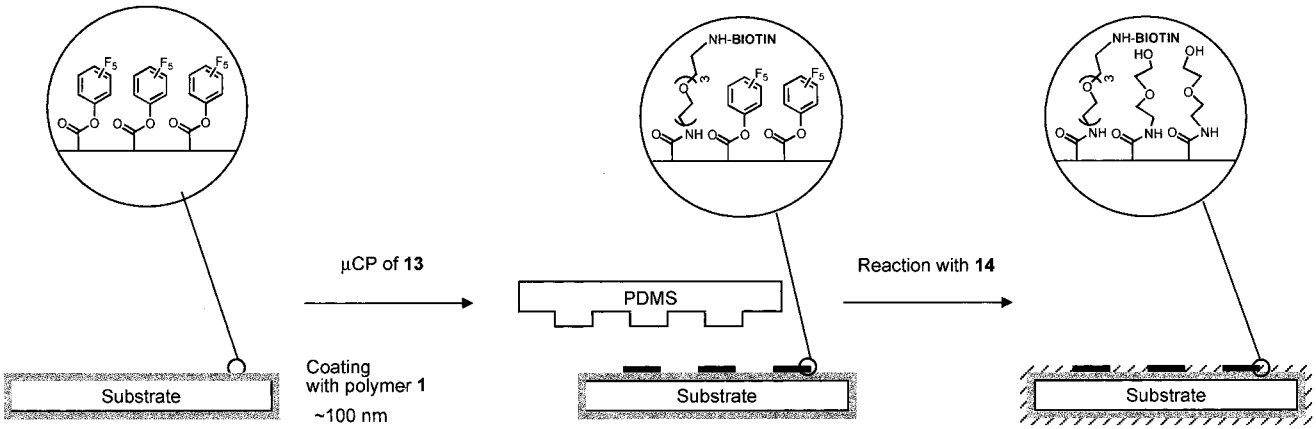

Figure 3. Representation of the process that was used for μCP of the amino-functionalized biotin ligand **13** onto reactive coatings **1** (shown as an example) and **2**. A PDMS stamp, manufactured as a replica from a silicon master, was used for printing ligand **13** onto polymer **1**. The remaining surface area was passivated by reaction with compound **14**.

with an Al Kα X-ray source. Pass energy was 160 eV for survey spectra and 10 eV for high-resolution spectra. All spectra were calibrated in reference to the unfunctionalized aliphatic carbon at a binding energy of 285.0 eV. Infrared (IR) spectroscopy was done on a Magna 550 spectrometer (Nicolet) equipped with a grazing angle accessory (Spectra-Tech) under a grazing angle of 85°. Spectroscopic ellipsometry was carried out on a variable angle spectroscopic ellipsometer (J. A. Woollam Inc., USA) using a Cauchy model for curve fitting. For both polymers, variation in thickness was below 8% over a sample area of 1 cm^2. For fluorescence microscopy, samples were rinsed well with PBS and examined with a HFX-DX fluorescence microscope (Nikon, Japan) and a computer-aided picture capturing system (IP-spectrum software).

2.5. Microcontact Printing. A polished 4-in. silicon wafer was spin-coated with a negative photoresist (SU8-100) and processed by photolithography to develop patterns on the wafer surface. Subsequently, the wafer was silanized by incubation with tri(decafluoro-1,1,2,2-tetrahydrooctyl)-1-methyldichlorosilane under vacuum for 2 h. To cast the PDMS stamps, the master was covered in a Petri dish with 50 g of PDMS oligomers (Sylgard 184 silicone elastomer). After curing for 6 h at 60 °C, the PDMS stamp was peeled off from the master.[28,29] Prior to use, the PDMS stamp was oxidized by means of an oxygen plasma (Harrick PDC-32 G, medium setting, 2 mbar) for 1 min. A cotton swab was wetted with a solution of (+)-biotinyl-3,6,9-trioxaundecanediamine (**13**) in ethanol (10 mM) and dragged once across the patterned side of the stamp. The stamp was dried with a stream of nitrogen for 20 s and pressed onto the sample surface for 60 s. The sample was immersed immediately in a solution of 2-(aminoethoxy)ethanol (**14**) in anhydrous dimethylformamide (10 mM) for 2 h. The sample was removed and rinsed with distilled water.

2.6. Immobilization of Human Anti-α_5-integrin. Patterned samples were incubated in sterile Petri dishes with phosphate buffered saline (PBS, pH 7.4) containing 0.1% (w/v) bovine albumin and Tween 20 (0.02% (v/v)) for 30 min and with a solution of streptavidin (10 mM) or fluorescein-conjugated streptavidin (10 mM) for another 60 min (all in PBS containing 0.1% (w/v) bovine serum albumin and 0.02% (v/v) Tween 20). The surface was rinsed several times with PBS and then exposed for 120 min to a solution of biotin-conjugated human anti-α_5-integrin (**15**, 6 μg/mL). The patterned samples were rinsed with PBS and transferred immediately to Petri dishes. For samples patterned with **15**, fluorescence staining was done by incubating with a solution of fluorescein-conjugated secondary antibody (fluorescein-conjugated anti-mouse IgG) dissolved in PBS (1:20) for 30 min.

2.7. Cell Experiments. BAEC were purchased from Cell Systems, WA, and cultured as described elsewhere.[30] Cells were seeded for 24 h in serum-free DMEM and fixed with 3% paraformaldehyde in Ca^{2+} and Mg^{2+} enriched PBS for 30 min at room temperature. Cell nuclei were stained with bis-benzimide in Ca^{2+}- and Mg^{2+}-enriched PBS (1:100). Immunofluorescent images were recorded on the above-mentioned fluorescence microscope.

3. Results and Discussion

We used CVD polymerization to prepare thin films of the reactive coating **1** and **2**. In contrast to polymer **1**, polymer **2** enables binding of biomolecules without releasing potentially harmful leaving groups such as pentafluorophenol. This is critical for applications in biology, as recent work revealed nonquantitative conversion of pentafluorophenol ester groups when modified by μCP.[22] We compared both reactive coatings with respect to their ability to support μCP of a biotin ligand and used these patterned substrates to spatially direct the adsorption of antibodies and the adhesion of cells.

3.1. Synthesis of [2.2]Paracyclophanes. Compound **6** was synthesized from [2.2]paracyclophane via a three-step synthesis.[26] As shown in Figure 1, [2.2]paracyclophane (**3**) was converted to 4-trifluoro[2.2]paracyclophane (**4**) by reaction with trifluoroacetic acid anhydride and aluminum chloride. Subsequently, compound **4** underwent base-catalyzed hydrolysis to yield 4-carboxy[2.2]paracyclophane (**5**). The final product **6** was synthesized from **5** by conversion with pentafluorophenol trifluoroacetate. [2.2]Paracyclophane 4,5,12,13-tetracarboxylic dianhydride (**12**) was synthesized from 4,5,12,13-tetrakis-(methyloxy carbonyl) [2.2]paracyclophane (**11**) by conversion with concentrated sulfuric acid (Figure 1). Compound **11** was obtained by Diels−Alder reaction of acetylenedicarboxylic acid methyl ester (dienophile, **10**) with hexatetraene (diene, **9**). Diene **9** was synthesized from compound **7** by reaction with allenylic magnesium bromide (**8**), which is accessible via Grignard reaction of compound **7**.[31] The synthesis was conveniently conducted at the 5-g scale with overall yields of 32%.

3.2. Preparation and Characterization of Reactive Coatings. The CVD process followed the procedure of Gorham[32−34] and allowed the preparation of homogeneously deposited films. As shown in Figure 2, reactive coatings **1** and **2** were prepared by pyrolysis of vaporized

(28) Lahiri, J.; Ostuni, E.; Whitesides, G. M. *Langmuir* **1999**, *15*, 2055.
(29) Kumar, A.; Whitesides, G. M. *Appl. Phys. Lett.* **1993**, *63*, 2002.
(30) Rosenthal, A. M.; Gotlieb, A. I. *Cell Cultue Techniques in Heart and Vessel Research*; Springer-Verlag: Berlin, 1990; pp 117.
(31) Hopf, H. *Angew. Chem.* **1972**, *84*, 471.
(32) Gorham, W. F. *J. Polym. Sci. Part A-1* **1966**, *4*, 3027.
(33) Gorham, W. F.; Yeh, Y. L. *J. Org. Chem.* **1969**, *34*, 2366.
(34) Simon, P.; Mang, S.; Hasenhindl, A.; Gronski, W.; Greiner, A. *Macromolecules* **1998**, *31*, 8775.

Table 2. Chemical Composition of CVD-Coated Gold Substrates in Atom %

		C_{1s}							O_{1s}		F_{1s}
	polymer	285.0 eV *C*-C	285.7 eV *C*−CO−O	286.7 eV *C*−O	288.9 eV C−*C*O−O	289.7 eV O−*C*O−O	290.6 eV C−F	291.7 eV $\pi\rightarrow\pi^*$	532.5 eV C=*O*	533.9 eV C−*O*	686.9 eV C−*F*
calcd	**1**	50	3.3	3.3	3.3		16.7		3.3	3.3	16.7
found		49.1	2.3	2.7	3.9		16.4	1.5	3.0	2.9	18.2
calcd	**2**	46.1		15.4		15.4			15.4	7.7	
found		50.0		13.8		12.3		0.9	15.1	7.9	

[2.2]paracyclophanes via *p*-quinodimethanes, which condensed onto the substrate and spontaneously polymerized. The low substrate temperature during the polymerization (<15 °C) allows coating of temperature-sensitive substrates (e.g., poly(lactic acid)) without decomposition. Conditions of quinodimethane creation in the pyrolysis zone are generally the bottleneck in determining whether a functional group is suitable for CVD polymerization. Thus, CVD polymerization of [2.2]paracyclophanes requires optimum adjustment of reaction conditions to minimize decomposition of the functional groups. The experimental setup allowed individual control of several polymerization parameters, such as pyrolysis temperature, pressure, gas flow, substrate temperature, and sublimation temperature.[27] We found the influence of the pyrolysis temperature to be most stringent for both chemical polymer composition and adhesion behavior. Pyrolysis was best conducted at a temperature below 670 °C as compared to 850 °C used for nonfunctionalized [2.2]-paracyclophane.[35] Thicknesses of polymer films **1** and **2** prepared according to polymerization data given in Table 1 were determined using spectroscopic ellipsometry to be 131 nm (for **1**) and 90 nm (for **2**). Deposited in thin films, reactive coatings showed excellent adhesion properties on substrate materials such as PE, PTFE, stainless steel, gold, or glass. Adhesion of the reactive coating to a substrate was examined by gently pressing a 1 cm^2 area of Scotch tape onto the polymer coating. After subsequently peeling off the tape, the sample was examined by optical microscopy and infrared spectroscopy and was mechanically and chemically intact. Similarly, coatings showed good stability when mechanically stressed with a cotton swab after incubation for 30 min in methylene chloride or acetone. The excellent adhesion properties of the two reactive polymers are in accordance with those of similar CVD polymers and are mainly driven by physical encapsulation of the underlying substrate.[36] Furthermore, reactive coatings were stable in a dry air atmosphere for several weeks. Both reactive coatings were insoluble in common solvents, e.g., dimethylformamide, ethanol, or aqueous solutions.

The chemical composition of polymers **1** and **2** were generally in good accordance with the theoretically expected values as determined by XPS (Table 2). However, the O:C ratio of 0.22 detected for polymer **2** was lower than the theoretically expected ratio of 0.30 indicating a potential decrease of functional groups. The C_{1s} spectrum revealed three different signals: (1) aliphatic hydrocarbon (*C*−C, *C*−H) at a binding energy of 285.0 eV, (2) a carbon in immediate neighborhood to the carbonyl group (*C*−CO−O) at 286.7 eV, and (3) a carboxy carbon (*C*=O at 289.7 eV). In addition, a weak signal at a binding energy of 291.7 eV indicated $\pi-\pi^*$ transitions that are characteristic for aromatic polymers.[37] The O_{1s} spectrum of polymer **2** was characterized by two signals at 532.5 and 533.9 eV detected at a ratio of 2:1. No signs for oxidative decomposition were found based on the high-resolution XPS. We further conducted elemental analysis on micrometer-thick polymer films isolated from a glass substrate that revealed a O:C ratio of 0.41 as compared to a theoretically expected value of 0.40. Thus, we concluded that superficial carbon impurities account for the decreased O:C ratio. To unambiguously verify the integrity of the functional groups in the reactive coatings, we used grazing angle infrared spectroscopy. The IR spectrum of polymer **2** is characterized by the double signal of the C=O stretching vibration at 1777.5 and 1849.2 cm^{-1} and characteristic bands of C−O−C stretching vibrations at wavelengths of 1177.9 and 1244.3 cm^{-1}, which show the intensity distribution typical for cyclic anhydrides. After establishing the chemical composition of the reactive coatings, we assessed their feasibility to support further surface modification by μCP.

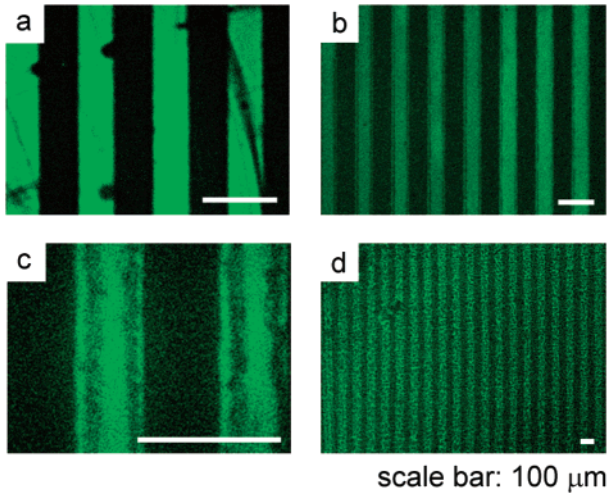

Figure 4. Fluorescence micrographs of PTFE coated with polymer **1** (a) and **2** (b) and gold coated with polymer **1** (c) and **2** (d) after μCP with ligand **13** and self-assembly of fluorescein-conjugated streptavidin. The width of each individual line is 50 μm.

3.3. Microengineered Surfaces. Surface patterns were achieved by (1) reactive coating, (2) patterning of amino-derived biotin ligands and (3) layer-by-layer self-assembly on patterned surfaces. Figure 3 represents the process of patterning substrates with a set of parallel lines of (+)-biotinyl-3,6,9-trioxaundecanediamine (**13**) having a width of 50 μm. The lines were separated by 50 μm wide regions of 2-(aminoethoxy)ethanol (**14**). Compound **14** covalently binds via amino groups to the surface and suppresses nonspecific adhesion of proteins and increases signal-to-noise ratios.[22] PTFE substrates coated with either polymer **1** or **2** and modified by μCP with ligand **13** were stored in an aqueous PBS buffer (pH 7.4) for 7 days at room temperature. Storage under these conditions did not affect the mechanical stability of the reactive coatings.

A biotin-based ligand was chosen because of its strong noncovalent interaction with streptavidin ($K_D = 10^{-15}$

(35) Schmidt, C.; Stuempfen, V.; Wendorff, J. H.; Hasenhindl, A.; Gronski, W.; Ishaque, M.; Greiner, A. *Acta Polym.* **1998**, *49*, 232.
(36) Greiner, A. *Trends Polym. Sci.* **1997**, *5*, 12.
(37) Gardella, J. A.; Ferguson, S. A.; Chin, R. L. *Appl. Spectrosc.* **1986**, *40*, 224.

M).[18−22,38,39] Self-assembly of streptavidin was studied on chemically distinct substrates such as PTFE, PE, gold, silicon, stainless steel, and glass, all coated with reactive coating **1** or **2**. Figure 4 shows PTFE and gold substrates coated with either polymer **1** or **2** after μCP of ligand **13**. Within the range of substrates in this study, the formation of patterns was independent from the substrate material. Samples were further incubated with fluorescein-conjugated streptavidin in the presence of Tween 20, a blocking agent composed of polyoxyethylene sorbitan monostearate that preferentially adsorbs to the background and suppresses unspecific adsorption of streptavidin.[21] Successful patterning was verified by fluorescence microscopy for PTFE (Figure 4a,b) and gold (Figure 4c,d). Both reactive coatings revealed similar results: streptavidin bound primarily onto biotin-coated regions. High accuracy with respect to contrast and pattern formation was found. In contrast, the fluorescence intensity of unmodified poly(*p*-xylylene), which was stamped following the same procedure, showed a significantly lower contrast between the patterned regions and the background.

3.4. Formation of Cell Pattern. Poly-*p*-xylylenes are promising candidates as cell templates due to their low intrinsic cytotoxicity. When previously reacted with albumin, reactive coatings **1** and **2** did not indicate short-term cytotoxicity. Our motivation was to assess whether the patterned polymer interfaces allows spatially defined self-assembly of antibodies that bind to features expressed on a cell surface and whether those antibodies could be used to guide cells to defined locations on the substrate. Cell adhesion is a specific process[40] that involves interactions between cell adhesion mediators (fibronectin, laminin, collagens, etc.) and cell surface receptors (CSRs) comprising cadherins, integrins, immunoglobulins, or selectins.[41,42] CSRs possess specific binding sites for extracellular matrix proteins, and their expression varies with cell type. While some CSRs are expressed almost universally (e.g., laminin receptors[43]), others are specific for a cell type. The fibronectin receptor VLA-5 is expressed only by a few cell types including endothelial cells, epithelial cells, platelets, and fibroblasts. VLA-5 is formed on the cell surface by association of β_1-integrin with α_5-integrin being itself a dimer of 135/25 kD. α_5-Integrin was chosen as a target for its role in cell adhesion and its relative specificity for endothelial cells. Our strategy was based on the hypothesis that a surface-bound antibody against the VLA-5 receptor fragment α_5-integrin (human anti-α_5-integrin) would initiate attachment of endothelial cells.

To verify this hypothesis, adsorption of biotin-conjugated human anti-α_5-integrin (**15**) on a prestructured surface was investigated. We used streptavidin as a linker by first allowing it to bind to the surfaces modified by μCP with biotin-ligand **13**. The use of streptavidin generates a universal platform for further attachment of biotin-conjugated proteins, since streptavidin has two pairs of binding sites on opposite faces. Two of its binding sites at one face were used to link the protein to the biotin-coated regions of the surface, leaving two binding sites on the opposite face for further attachment. Self-orientation was induced by simply immersing a streptavidin-patterned sample in a solution of antibody **15** for 2 h. Surface-bound antibody **15** was marked with a fluorescein-conjugated secondary antibody that recognizes the heavy chain of antibody **15**. Figure 5 shows fluorescence micrographs of the two reactive coatings after spatially controlled immobilization of antibody **15** and subsequent association with the secondary antibody. The fluorescein-labeled secondary antibody was found to bind only at areas patterned with antibody **15**. Figure 5 reveals sharp contrast between binding and nonbinding regions. The micrograph also demonstrates homogeneous and reproducible distribution of antibody **15** on the biotin-terminated areas of the surface.

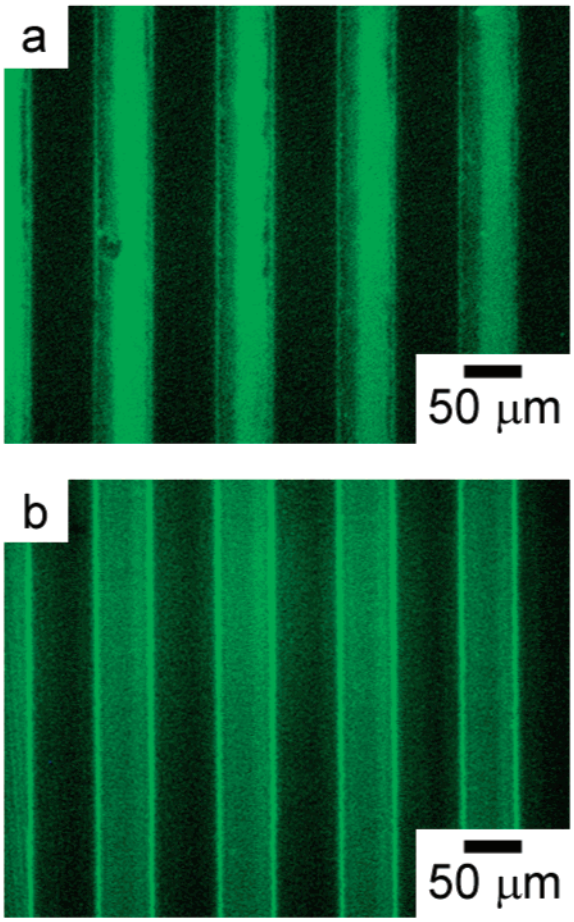

Figure 5. Fluorescence micrographs of (a) a gold substrate coated with polymer **1** and patterned with antibody **15** and (b) a PTFE substrate coated with polymer **2**, both patterned with antibody **15.** Both samples were immunoassayed with a fluorescein-labeled secondary antibody against **15**. The width of each individual line is 50 μm.

We then used gold surfaces to study a spatially directed cell attachment. Surfaces exposing patterns of antibody **15** were incubated with a suspension of bovine aortic endothelial cells (BAECs) in serum-free Dulbecco's modified eagle medium (DMEM). Since our goal was to study initial cell attachment, cells were immersed for 24 h with the patterned surfaces. With substrates patterned into regions that alternately promote or prevent the binding of antibody **15**, attachment and spreading of BAECs were controlled. Cell attachment was studied by means of immunofluorescence microscopy and light microscopy and revealed high contrast between patterned areas and the background (Figure 6). We further examined the reproducibility of the method over wider areas by stamping an

(38) Birkert, O.; Haake, H. M.; Schutz, A.; Mack, J.; Brecht, A.; Jung, G.; Gauglitz, G. *Anal. Biochem.* **2000**, *28*, 200.
(39) Haeusling, L.; Michel, B.; Ringsdorf, H.; Rohrer, H. *Angew. Chem., Int. Ed.* **1991**, *30*, 569.
(40) Genui, E.; Granchi, D.; Cipetti, G.; Verri, E.; Cavedagna, D.; Gamberini, S. Cervellati, M.; DiLeo, A.; Pizzoferrato, A. *Biomaterials* **1997**, *18*, 489.
(41) Frenette, P. S.; Wagner, D. D. *N. Engl. J. Med.* **1996**, *334*, 1526.
(42) Huttenlocher, A.; Sandborg, R. R.; Horwitz, A. F. *Curr. Opin. Cell Biol.* **1995**, *7*, 697.
(43) Delwel, G. O.; Sonnenberg, A. *Adhes. Recept. Ther. Targets* **1996**, 9.

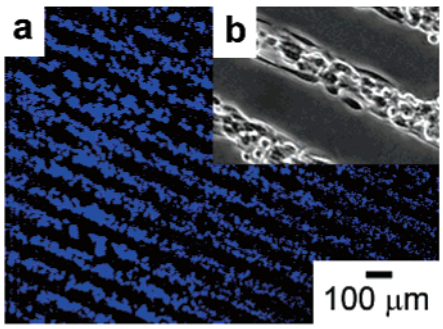

Figure 6. (a) Fluorescence micrograph of BAEC seeded for 24 h on a gold substrate (cell nuclei were stained with bisbenzimide). (b) Enlargement of optical micrograph of BAEC seeded for 24 h on a gold substrate. In all cases, the substrate was previously coated with polymer **1** and patterned with ligand **13** to control self-assembly of antibody **15**. The width of each individual line is 50 μm.

area of ca. 1 cm^2 of polymer **1**. A representative image is shown in Figure 6 that indicates uniformity of the pattern over the entire stamped region. Little loss of feature resolution and intensity was detected at the edges of the stamped regions, which is important for applications such as bioassay development. In addition, high cell densities of BAECs were found for areas coated with antibody **15**, whereas BAECs did not attach to areas that did not present antibody **15** (background). Cell densities were twice as large as found for tissue culture polystyrene that was incorporated as reference material in this study. We then concluded that the surface properties are completely determined by the reactive coating and that μCP of biotin ligands issues control over the adsorption behavior of streptavidin.

4. Conclusions

The main significance of this study is to demonstrate the feasibility of CVD polymerization for synthesizing chemically and topologically uniform reactive polymer coatings. These submicrometer-thin coatings are characterized by functional groups with high chemical reactivity, e.g., anhydride or pentafluorophenol ester groups. Applicability of reactive coatings to various substrates, such as polymers or metals, generates a fairly universal platform without relying on chemical alteration of the bulk material. When comparing reactive coatings **1** and **2**, their applicability for surface engineering is similar despite the different chemical nature of their functional groups enabling different binding characteristics with biomolecules.

Furthermore, the use of these surfaces as templates for layer-by-layer self-assembly of proteins and cells presents a path toward spatially directed cell attachment. In this study, we focused on initial cell attachment within 24 h, a time range that is believed to be crucial for microfluidic devices or biosensors. Nevertheless, a more comprehensive insight in the stability of cell patterns will benefit from studies using serum-containing medium over longer time ranges. We exploited antibodies against a cell-specific integrin to initiate the formation of cell patterns. Although used in this study in a noncompetitive mode, the use of cell-specific antibodies may constitute a first step toward coattachment of different cell types. This is the case when different cells follow a pattern that is created by surface-confined antibodies that bind selectively to a specific cell type.

In summary, reactive coatings have proven to be a promising platform to study correlations between surface parameters and cell attachment. While overcoming restrictions associated with gold/alkanethiolates-based soft lithographic techniques, the technology maintained intrinsic advantages of soft lithography, e.g. accuracy, broad availability, and low costs.

Acknowledgment. This work was supported by the Fonds der Chemischen Industrie, the National Science Foundation, and the National Institutes of Health. I. S. Choi thanks the Korea Science and Engineering Foundation and the Brain Korea 21 Project for financial support.

LA011464T